Gold Nanoparticles Protected by Fluorinated Ligands: Syntheses, Properties and Applications

Paolo Pengo[a] and Lucia Pasquato[a,b,*]

[a] Department of Chemical and Pharmaceutical Sciences, University of Trieste, 34127 Trieste, Italy.

[b] INSTM, Trieste Unit, Trieste Italy.

Email: lpasquato@units.it

Department of Chemical and Pharmaceutical Sciences, University of Trieste, Via L. Giorieri 1, 34127 Trieste, Italy. Phone: +390405882406; FAX: +390405883903.

Keywords: Fluorinated gold nanoparticles, fluorinated monolayers, mixed monolayers, molecular recognition, drug delivery, theranostics.

Abstract:

The development of fluorinated gold nanoparticles is presently arising and increasing attention across several fields of nanotechnology. The synthetic approaches evolved over time from the use of almost perfluorinated alkanethiols and perfluorinated arylthiols to amphiphilic fluorinated thiols capable of ensuring solubility in conventional organic solvents and water. The interest in these systems stems from the unique properties of both nanosized and fluorous compounds. In perspective, the development of our understanding of the fluorophilic interactions at the nanoscale will allow to devise novel strategies for self-assembly, molecular recognition and new materials for biomedical applications. In this paper we present, through selected examples, the potential of fluorous ligands in the synthesis of gold nanoparticles and the relevance of mastering the properties of these systems in the development of new materials.

Introduction

Gold nanoparticles with sizes in the range of 1-100 nm protected by a monolayer of chemisorbed thiolates are the subjects of intense research because their size-dependent properties enable a rich variety of novel materials to be obtained. This interest spans different fields of nanotechnology and material sciences, from self-assembly of higher order structures [1], catalysts [2] and sensors

development, to applications in the medical field [3] such as delivery of therapeutics [4-6] and diagnostics [7,8]. This popularity is certainly bound to their ease of preparation and functionalization; by the possibility of manipulating these systems like common organic compounds and, moreover, by the possibility of using conventional analytical techniques for their purification and characterization. These properties stem from the stability of the monolayer that protects, or passivate, the particles, which also dictates much of the chemical behavior of these systems in their interactions with other species. From this viewpoint, gold may be considered a convenient choice, making gold nanoparticles an easily accessible model to study the monolayer chemistry of nanosized objects. Historically, the first reliable synthesis of gold nanoparticles protected by an organic monolayer of thiolate ligands was developed by Brust and Schiffrin [9]. They reported the formation of monolayer protected gold nanoparticles by reduction of $HAuCl_4$ with sodium borohydride in the presence of excess dodecanethiol and tetraoctyl ammonium bromide as phase transfer agent. The homoligand systems obtained were stable in solution and in the solid state and freely soluble in common apolar solvents. The second major step in gold nanoparticles chemistry come after the discovery of the place exchange reaction [10] by R. W. Murray and coworkers that enabled the introduction of a rich variety of functional thiolates in the monolayer of preformed nanoparticles. Virtually any functional group can be introduced in the monolayer of gold nanoparticles by this method. This is particularly useful when functional thiols cannot be used in the Brust-Schiffrin procedure; either because of limited stability under reducing conditions or because synthetic limitations hamper the use of the excess thiol needed in the direct synthesis. In the mixed monolayer nanoparticles obtained the ligands could be arranged in a random distribution, essentially maximizing the entropy of mixing, or, on the contrary, may form segregated domains. This was actually found to be true under well-defined geometric and thermodynamic constraints [11,12]. The formation of monolayer domains made of different thiolates is a source of chemical anisotropy on an otherwise very symmetric surface. This is the starting point to devise nanoparticles based building blocks to assemble (or to induce the self-assembly of) higher order structures in a predictable and programmable manner. In this respect, extreme phase segregation can be achieved by exploiting the tendency of fluorocarbon chains (F-Chains) and hydrocarbon chains (H-Chains) to self-sort. Homoligand or heteroligand fluorous nanoparticles, however, may display markedly low solubility in common solvents, posing severe limitations to their purification, characterization and applications. To overcome this problem, the fluorinated moieties need to be shielded from the bulk solvent by using suitably solubilizing units with the penalty of an increased

synthetic effort. These systems are ideal models to analyze the scope of using fluorinated nanoparticles in solvent systems such as water or biological media that would have been otherwise inaccessible.

"Perfluorinated" gold nanoparticles

Early attempts of synthesis of nanoparticles by using heavily fluorinated alkanethiols, typically the commercially available 1*H*,1*H*,2*H*,2*H*-perfluoro alkanethiols and pentafluorobenzenethiol led to materials of very low solubility that proved to be difficult to purify and characterize. Among these early attempts, the first preparation of perfluorinated silver nanoparticles was reported by Korgel [13] in 2000 by using **1** in a modified Brust-Schiffrin procedure. Later, the synthesis of gold (and silver) nanoparticles was reported by Yonezawa and Kimizuka [14,15] in 2001 by using a single phase (ethanol) method in the presence of **1** or **2**, Figure 1. The material obtained precipitated off the solution because of the poor solvating properties of ethanol for these systems. The nanoparticles' core had a mean diameter of 2.4-2.6 nm and these systems were essentially insoluble in several organic solvents while they were readily soluble in fluorocarbons including hexafluorobenzene, perfluorobutylalkyl ethers and in HCFC225 (mixture of $CF_3CF_2CCl_2H$ and CF_2ClCF_2CClFH).

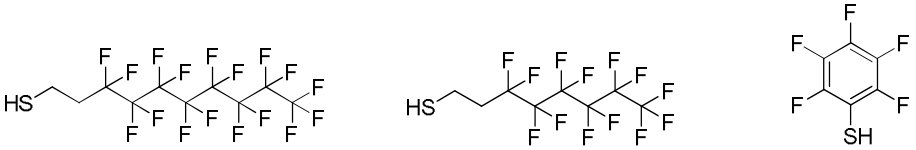

1 **2** **3**

Figure 1. Structures of the (quasi) perfluorinated alkanethiols and aryl thiols used in the early synthesis of fluorinated gold nanoparticles.

The characterization of the nanoparticles by TEM analyses revealed a narrow size distribution with a strong tendency of forming 2D superlattices onto the TEM support. The gap between adjacent gold cores in the 2D-lattice was smaller than twice the length of the thiolate ligand, with strong indication that self-assembly was led by interdigitation of F-chains of neighboring particles. Other early examples of perfluorinated nanoparticles of smaller size, comprising 44-75 gold atoms in their core were reported by Murray and coworkers [16]. These nanoparticles were prepared by two different synthetic methods: i) the reaction of **1** with tetrachloroauric acid in a typical Brust-Schiffrin procedure and ii) by reaction of the molecularly precise gold cluster $Au_{55}(PPh_3)Cl_6$ with pentafluorobenzenethiol **3**. As observed by Yonezawa, the materials obtained displayed solubility only in fluorocarbons. In the preparation of

nanoparticles according to the Brust-Schiffrin method, that employs tetraoctylammonium bromide as phase transfer agent, the authors observed a significant reduction of the solubility by increasing the number of washing cycles needed to remove the excess phase transfer agent. This was a clear indication that the fluorous nanoparticles were able to trap this species, a behavior never reported for hydrogenated nanoparticles. However, it was not clear whether the ammonium ion was adsorbed in the monolayer or entrapped in the nanoparticles precipitate. Such a distinction is crucial because in the former case it would have indicated the tendency of fluorinated nanoparticles to take place in molecular recognition events, in spite of the tendency of fluorocarbons and hydrocarbons to form separate phases. In the synthesis reported by Murray the nanoparticles' size was much smaller than that obtained by Yonezawa, but was still polydispersed as could be inferred from UV-Vis analysis. In the preparation that employed the Au_{55} template, the structural integrity of the cluster was not retained and the reaction occurred with the formation of larger particles, including Au_{75} clusters, identified by voltammetric techniques because of its typical band gap. This behavior was not directly due to the fluorinated thiols because it was also observed with hydrogenated alkanethiols [17]. An application of these perfluorinated nanoparticles was reported by Whitten [18]: thin films of 1*H*,1*H*,2*H*,2*H*-perfluorodecanethiolate protected gold nanoparticles were proved to uptake solvents in the vapour phase with a selectivity order: Hexafluorobenzene > methanol > hexane > chloroform > toluene = water. The electrical resistance of the nanoparticles' film decreased with vapor exposure, while the opposite behavior was observed with mercaptohexadecanic acid protected nanoparticles used as reference. The authors attributed this behavior to the porous structure of the film, resulting from the large inter-particle distance and the vapor-induced changes in film morphology. Besides the precise mechanism of vapor absorption, this was an early indication of the tendency of fluorinated gold nanoparticles to enter into selective molecular recognition events. These examples demonstrated the possibility of using fluorinated thiols in the synthesis of gold nanoparticles, while little attention was paid to the synthesis of small molecular clusters. Indeed, as yet, there are very few examples of small noble metal clusters protected by fluorinated ligands, with the notable exception of three $Ag_{44}(SR)_{30}$ and three $Au_{12}Ag_{32}(SR)_{30}$ intermetallic nanoclusters stabilized with fluorinated arylthiolates (SR=SC_6H_5F, $SC_6H_4F_2$ or $SC_6H_5CF_3$) [19]. The poor solubility properties of perfluorinated nanoparticles are certainly a limit but represent also an opportunity of studying the chemistry of gold nanoparticles in fluorocarbons or supercritical CO_2 (Sc CO_2). Indeed silver nanoparticles protected by **1** were found to be soluble in Sc CO_2 [13] with solubility increasing with the increase of Sc CO_2 density. Theoretical investigations confirmed these data and revealed that increasing the length of the fluorous

ligands could provide a strategy to devise more easily dispersible systems in Sc CO_2 [20]. Supercritical CO_2 also proved to be a good solvent for fluorous nanoparticles synthesis by using suitable organometallic precursors and hydrogen as reducing agent [21,22].

Fluorous gold nanoparticles with improved solubility properties

The solubility and purification issues of perfluoroalkyl protected gold nanoparticles severely limit the application of these systems. To address this problem several groups including ours were prompted to develop amphiphilic protecting thiolates with intrinsically ameliorated solubility properties. The strategy we devised was to append a PEG unit of variable length to a rigid fluorinated moiety bearing the thiol group necessary for grafting on the gold surface. The length of the PEG unit could be tuned allowing to identify the smaller number of oxoethylene units necessary to confer to the nanoparticles a significant solubility in polar media, thiols **4a**-**4d** [23], Figure 2.

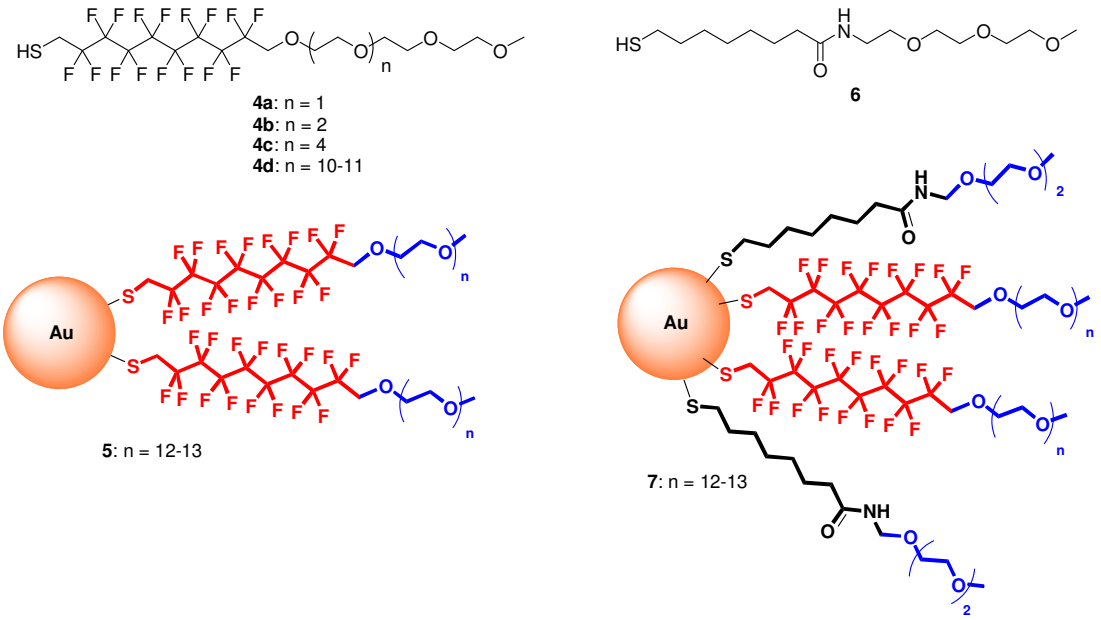

Figure 2. Structures of the amphiphilic thiols and fluorinated nanoparticles with solubility in polar solvents.

The development of the PEG functionalized fluorinated alkanethiols **4d** led, for the first time, to the synthesis of the fluorous gold nanoparticles **5** with solubility in a broad spectrum of common organic solvents and water [24]. In this case a single phase methodology was devised for the synthesis, limiting the use of any species interfering in the purification process. However, the thiol groups of these ligands

suffer of a markedly reduced nucleophilicity. This results from the electron-withdrawing effect of the fluorinated chain in the α position with respect to the sulfur atom; in the nanoparticles synthesis we were forced to use the thiolate anion instead of the thiol. This effect was never observed with 1*H*,1*H*,2*H*,2*H*-perfluoroalkanethiols, indicating that two methylene groups are sufficient to temper the electron withdrawing effect of the F-chain. Despite this property of ligands **4a**-**4d**, the X-Ray Photoelectron Spectroscopy (XPS) analysis of nanoparticles **5**, confirmed the presence of metallic Au atoms on the last shell, in keeping with the observations on alkanethiolate protected gold nanoparticles. In closed details, the Au 4f core level of nanoparticles **5** appears as the typical metallic doublet with a $4f_{7/2}$ binding energy of of 83.95 eV, the presence of a significant population of oxidized gold atoms, (Au(I)), would have led to the presence of a peak at about 1 eV higher binding energies [25]. In general there are limited data available on the effect of the electron density on the thiol on the stability of the nanoparticles, while the stability was clearly correlated with the formation of a compact monolayer [26]. The nanoparticles **5** were found to be as stable as their hydrogenated analogues and displayed the expected reactivity in the place exchange reaction. Indeed, the nanoparticles **5** could be functionalized with thiol **6**, allowing the preparation of heteroligand nanoparticles **7** featuring hydrogenated and fluorinated chains in the proximity of the gold core. A somewhat similar strategy to fluorous nanoparticles with improved solubility in organic solvents was reported by Niikura [27,28] that developed the gold nanoparticles **8** and **9** functionalized by thiolates featuring a short perfluoroether moiety, Figure 3.

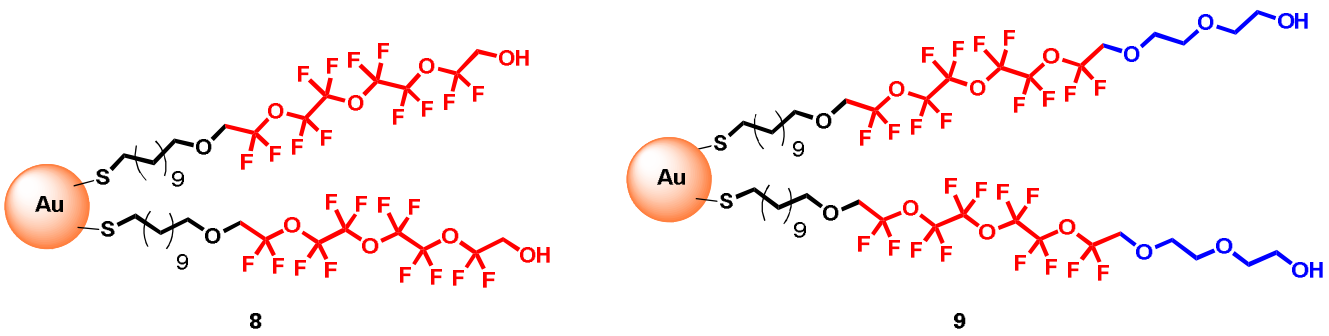

Figure 3. Structures of the fluorinated nanoparticles systems reported by Niikura [27,28].

In this case the fluorinated unit was not shielded from the solvent bulk, and this resulted into interesting self-assembly properties of the systems, that will be described below, but did not confer solubility in water to the nanoparticles.

Fluorous monolayers in 3D: host-guest chemistry, monolayer structure, assembly properties and applications.

The improved solubility properties of the nanoparticles **5**, **8** and **9** paved the way to a series of studies inaccessible to perfluoroalkanethiolate protected gold nanoparticles aimed at gaining information on the host-guest chemistry of homoligand fluorinated monolayers in comparison with hydrogenated monolayers of similar structure or of heteroligand (mixed) monolayers. In addition, accessibility of polar solvent systems, water and biological media enables the use of these nanoparticles systems in biomedical applications.

Host-Guest Chemistry

The nanoparticles monolayer is responsible for the large majority of the interactions with other species. The monolayer may be designed to display functional groups on its outer surface for specific molecular recognition: in this case the nanoparticles act as exo-receptors. On the other hand, the monolayer of unfunctionalised nanoparticles displays host-guest chemistry in its own right. In nanoparticles **5** and **7**, the inner part of the monolayer, close to the gold surface, is hydrophobic (because of the presence of H- or F-alkyl chains) while the outer part is considerably more hydrophilic to ensure solubility in polar media. In addition, in the case of nanoparticles **7** protected by mixtures of H-/F-ligands, mixed monolayers displaying the formation of domains are observed. This finding has two important implications: (i) the clustering of fluorous ligands on the nanoparticles' surface may be exploited to present a high density of functional groups for applications in multivalent molecular recognition and catalysis, and (ii) the clustering of fluorous ligands results in the formation, within the same monolayer, of several compartments with different hydrophobic properties. This last feature makes the monolayer of gold nanoparticles an interesting system for the non-covalent entrapment of small organic molecules. In this context we actively pursued the thermodynamic analysis of the complexation of organic nitroxides with the monolayer of gold nanoparticles by ESR spectroscopy, [24,29,30], Figure 4. The nitroxide radicals present two different mesomeric structures and the magnitude of the hyperfine coupling constants of the nitroxide radicals is a measure of the polarity of the environment experienced by the probe. It is this feature of that allowed assessing, for the first time the formation of segregated domain in the monolayer of nanoparticles **7**.

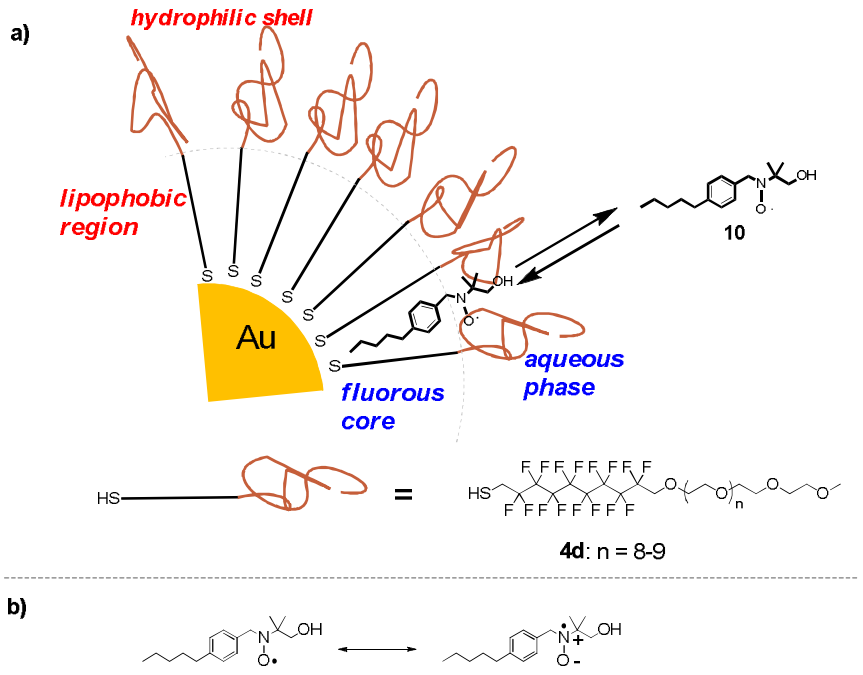

Figure 4. a) Partition equilibrium of the radical probe **10** between water and the monolayer of nanoparticles **5**; b) mesomeric forms of the radical probe **10**.

In addition, in a typical ESR experiment it is possible to monitor both the bound and unbound nitroxide species, allowing the easy determination of the partition constant of the probe for the monolayer. This approach allowed for the first time to evidence that nanoparticles **5** act as better hosting systems than hydrogenated nanoparticles of similar structures made by using thiol **6**. The binding constant of the radical probe **10** for the monolayer of nanoparticles **5**, Figure 4, was 176 M^{-1} while for the hydrogenated monolayer of nanoparticles with the same size, the binding constant was estimated to be 87 M^{-1}. This almost twofold increase is due to the enhanced hydrophobicity of the fluorous nanoparticles respect to the hydrogenated ones. Geometric considerations are also important because the larger inter-chain room available in fluorous monolayers allows for a smaller reorganization of the monolayer upon binding of the probe. In a recent study [31] we further expanded this analysis by considering the two structurally different water-soluble homoligand gold nanoparticles **5** and **11b**, Figure 5. This study was aimed at gaining some fundamental information about the relevance of fluorophilic interactions in the determination of the binding constant of nanoparticles towards small organic molecules. While nanoparticles **5** feature a rigid fluorous monolayer in the proximity of the gold core, nanoparticles **11b** feature a flexible fluorinated region at a distal position. These two

nanoparticles systems were compared to nanoparticles **12** of the same size. In this analysis a series of hydrogenated and fluorinated radical probes was considered.

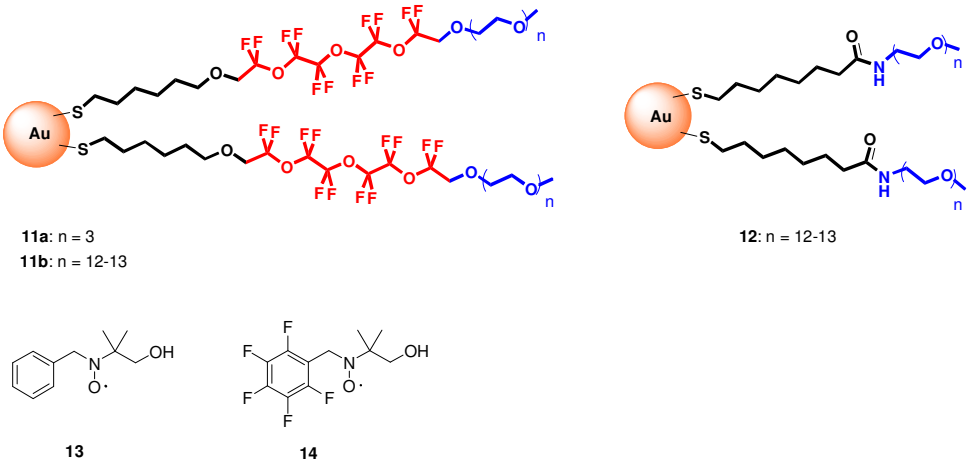

Figure 5. Structures of the fluorinated water-soluble gold nanoparticles featuring fluorinated units distal to the gold surface and an example of radicals probes used in this study, [31].

The comparison of the data obtained for nanoparticles **5** and **11b** with the binding behavior of hydrogenated nanoparticles **12**, revealed that fluorous monolayers act as better hosting systems for both hydrogenated and fluorinated guests. In addition, the flexible fluorinated monolayer of nanoparticles **11b** acts as a better hosting system than the more rigid counterpart **5**. As an example of the relevance of fluorophilic interactions, the binding constants of the two structurally similar radicals **13** and **14** for the monolayers of nanoparticles **11b** were 6.2 M^{-1} and 80 M^{-1} respectively. Fluorinated monolayers also displayed significant binding of hydrophobic, non-fluorinated guests which seems counterintuitive and at odd with the behavior of bulk fluorous phases. However, soluble nanosystems such as the nanoparticles described need to be considered associated with their solvation shell and with the differential solvation of the different monolayer environments. From this viewpoint, it is not surprising that the poorly solvated flurous regions could be better stabilized by interaction with hydrophobic species rather than water. These systems are of considerable interest because several FDA approved drugs, comprising anti-cancer drugs, contain one or more fluorine atoms, and an understanding of the basic principles of monolayer design aimed at maximizing the binding of these species are at the basis of the development of novel fluorous drug delivery systems.

Monolayer structure

The morphology of a mixed monolayer is the result of a complex interplay of different factors, including the nanoparticle size and the "likeliness" of the thiolates comprising the monolayer. Glotzer theoretically demonstrated that a length mismatch between two dislike thiolates is sufficient to drive the formation of stripe like domains on the surface of gold nanoparticles of diameters in the range 2.5-8.0 nm [32]. For smaller particles the formation of the so-called Janus particles is favored, with the two dislike ligands segregated on two hemispherical surfaces. The picture can be even more complicated when a blend of three or four dislike thiolate is considered [33,34]. The formation of these "patchy" particles is particularly interesting in the development of nanoparticles based building blocks for the assembly of higher order structures. To achieve these systems, the known tendency of F- and H-chains to self-sort represents a handy synthetic strategy. However, only few analytical techniques are practicable to map the nanoparticles surface thus providing direct evidence of the correctness of this approach. Direct structural information on the monolayer morphology can be obtained by Scanning Tunneling Microscopy (STM) analysis but this methodology is not suitable for the characterization of nanoparticles featuring long and flexible ligands. Indirect methodologies are however available, and ESR spectroscopy proved to be a useful tool in investigating the microenvironment of the monolayer and, as a consequence, provides useful information on the organization of the monolayer.

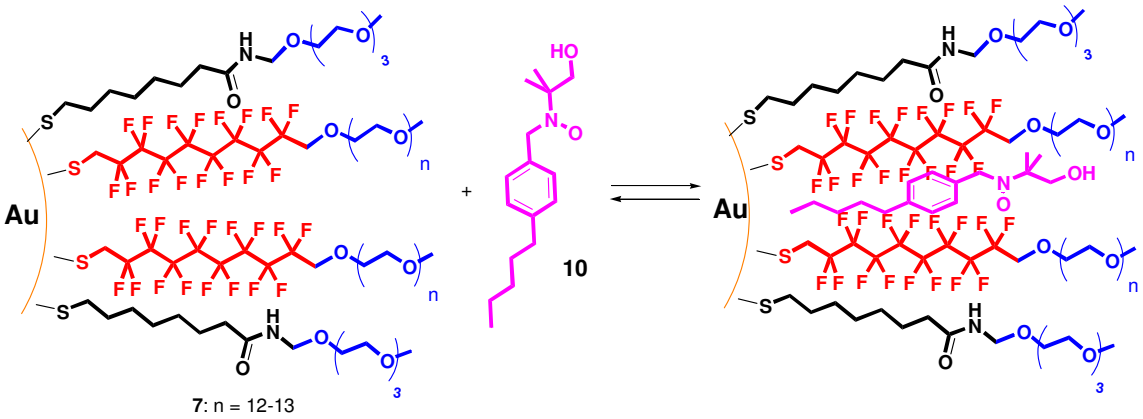

Figure 6. Partition equilibrium of the radical probe **10** between water and the mixed monolayer of nanoparticles **7**. The probe is preferentially complexed by the fluorinated domains of the particles.

In the case of mixed monolayer nanoparticles **7**, it was possible to highlight that the radical probe **10** experiences the environment of the fluorous phase even at very small loading of the fluorinated thiols, Figure 6, confirming the formation of small domains in keeping with the self-sorting characteristics of

the F and H- chains. Therefore on the surface of nanoparticles displaying hydrogenated and fluorinated ligands, phase separation occurs forming islands of homoligands triggered by the lipophobicity of perfluorocarbons. This represented the first example of a multicompartment water-soluble 3D SAM composed of two hydrophobic but immiscible components [29]. This system has potential for storage and release of two, or more, active but incompatible agents. A very interesting finding is that in the mixed monolayer nanoparticles **7**, the binding constants of small organic molecules for the fluorous phase increases with the decreasing the loading of the fluorinated component [30]. The experimental data were corroborated by multiscale molecular modeling indicating that, in mixed monolayers, the PEG units of the thiol **4d** bend over the shorter hydrogenated thiol, leaving more room around the F-chain. These findings can be summarized in a design tool: the spontaneous organization of the F-/H-chains in the inner part of the monolayer is transferred to the outer surface of the NP. Hence the properties of the mixed monolayer may be markedly different from those characterizing the parent homoligand monolayers. The multiscale molecular modeling also allowed analysis of the organization of the ligands in the monolayer as a function of the monolayer composition and nanoparticles' size. Indeed, in the presence of an equimolar mixture of the two ligands and for nanoparticles with a gold core of 2.2 nm, the H- and F-chains phase segregate into alternate domains with stripe morphology, extending along the diameter of the nanoparticles. Smaller nanoparticles with a gold core of 1.6 nm in diameter and the same composition, present a monolayer no longer organized in stripe-like domains but, instead, complete segregation occurs, with formation of a Janus nanoparticle. At lower loading of the fluorinated ligand, "patchy" particles are obtained.

Assembly properties

Niikura and coworkers reported the preparation of the 20 nm gold nanoparticles **8**, Figure 3, by using a fluorinated thiol featuring a perfluoropolyether moiety exposed to the solvent. These systems displayed an enhanced solubility in polar solvents including alcohols and THF [27]. STM analyses of the nanoparticles deposited on carbon-coated TEM grids revealed a strong tendency to form ordered superlattices on a long range (10 μm) with the formation of a hexagonally-packed and layered structure (3D-supperlattice). Structurally similar nanoparticles featuring only polyethylene glycol on their surface, instead, did not display any tendency to form ordered assemblies. The tendency of forming ordered structures was also function of the size of the particles, with smaller particles (5 nm in diameter) requiring solvents with higher boiling point and slower evaporation rates to achieve an ordered structure with respect to the larger ones. The authors explained this behavior by the self-

lubricating properties of the nanoparticles; these self-lubricating properties are the result of the low nanoparticles friction. This property could be of interest in using ink-jet processes or spin coating for the preparation of well-ordered and structured arrays of nanoparticles.

A self-assembly approach mediated by fluorophilic interactions was exploited by Niikura to develop sub-100 nm hollow superstructures. The nanoparticles building blocks **9**, Figure 3, display semifluorinated oligo(ethylene glycol) units in their monolayer and the self-assembly in vesicle-like structures was achieved without the need of any templates [28]. In this system the ligands are bundled on the surface of the nanoparticles and interact with ligands of other nanoparticles to form the structural element responsible for the formation of the hollow structure, Figure 7. These superstructures were formed in THF and, after assembly, could be transferred to other solvents including methylene chloride, ethyl acetate and butanol. Once formed the structures remain stable because of the solvophobic nature of the ligand bundles on the surface of the nanoparticle.

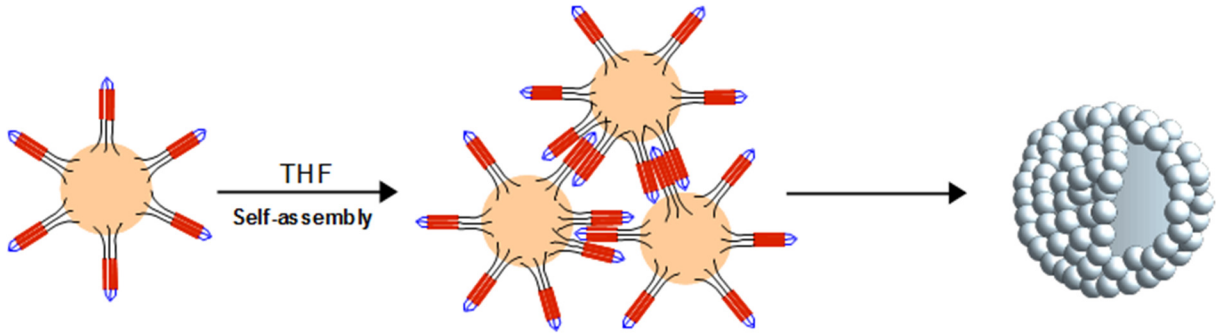

Figure 7. Proposed assembly mechanism for the nanoparticles **9** into spherical hollow superstructures.

Assembly by halogen bonds

An interesting opportunity for self-assembly offered by the use of fluorinated monolayers is the possibility of exploiting halogen bonds formation. Van der Boom [35] reported that the functionalization of gold nanoparticles with halogen bond donors allows the assembly of gold nanoparticles on quartz and silicon substrates functionalized with halogen bond acceptors. The morphology of the films was found to depend on the structure of the cross-linker and on the number of deposition steps. The assembled systems in the solid state displayed surface enhanced Raman scattering, with potential application in sensing. The same assembly properties could also be observed in solution, with formation of nanoparticles aggregates upon addition of multivalent halogen bond acceptors acting as crosslinkers. This study displayed for the first time that the formation of well-

defined nanoparticles assemblies based on the formation of interparticles halogen bonds is a practicable strategy.

Applications of fluorous nanoparticles

Several applications of fluorous gold nanoparticles described in the current literature are pertinent to the development of innovative diagnostic and therapeutic approaches. The recent trend is also to design novel theranostic agents merging the therapeutic and diagnostic functions into a single entity. These systems allow, for instance, to gain real-time information on the trafficking of the therapeutic species or to deliver a given pharmaceutical ingredient during the diagnostic procedure, knowing precisely where this is released. Gold nanoparticles are particularly fit to this approach because they can be functionalized with reporter units capable of being externally addressed, thus providing a diagnostic handle, and because the nanoparticles can be loaded with specific drugs. This second aspect is closely related to the binding properties of the monolayer discussed in the preceding sections. In this respect, fluorous phases present several advantages over hydrocarbon phases; indeed, the binding constants of drug-like molecules are higher for fluorous nanoparticles with respect to hydrogenated analogues [31]. Secondly, fluorinated nanoparticles may also act as reporter units by themselves, owing to the presence of the magnetically active ^{19}F nuclei that can be exploited in developing ^{19}F MRI contrast agents [36]. In principle, these two aspects led to a significant advantage in using fluorous instead of hydrocarbon phases, balancing the higher cost of fluorous building blocks with respect to hydrogenated analogues. An interesting approach to nanoparticles based drug delivery systems was described by Niikura [37]. By functionalization of the nanoparticles vesicles earlier reported by this author by using a PEG dithiol, the system was rendered water-soluble, providing, at the same time, cross-linking between the different particles in the construct. In this reaction the structure of the vesicle was maintained confirming the strength of the fluorophilic interaction at the basis of the self-assembly of the structure. This cross-linked structure proved to be dynamic under high temperature conditions and amenable of loading with the fluorescent dye rhodamine or with doxorubicin, an anticancer drug. This system was readily internalized by cells and the release of the encapsulated drug could be triggered by laser irradiation at 532 nm that allows the opening of the gaps between the particles [37]. Therefore this system may be considered a light-responsive drug delivery carrier for application in the biomedical field.

As mentioned above, another potential application of fluorinated nanoparticles in the biomedical field is related to the magnetic properties of the ^{19}F nucleus that has 100% natural abundance and sensitivity similar to that of ^{1}H. This makes fluorocompounds and fluorous gold nanoparticles extremely

interesting in magnetic resonance imaging with the additional benefits that ^{19}F-MRI analyses do not suffer of interferences from the background signal and allow quantitative determinations. To this end the gold nanoparticles **11a** and **11b** with quasi equivalent fluorine atoms were synthesized and analyzed in phantom experiments using a clinical setup [36]. With the nanoparticles **11a**, a signal to noise ratio of 5.7 could be obtained using a concentration of nanoparticles equal to 1.9 mg/ml. In addition, the capability of these systems to complex small drug-like organic molecules [31] enable to contrive their use as drug delivery vehicles that can be monitored in their action, representing an approach to gold nanoparticles based theranostics. A similar approach to gold nanoparticles based ^{19}F-MRI contrast agents and theranostics was developed by Williams and coworkers [38]. These authors reported the self-assembly of fluorinated amphiphiles bearing a guanidinuim moiety on the surface of gold nanoparticles featuring phosphonate groups. The same nanoparticles were decorated with gadolinium complexes [Gd(DOTA)] making the whole system paramagnetic. An interesting application of fluorinated gold nanoparticles in the analysis of biological materials was reported by Kraft and coworkers [39]. These authors exploited the fluorinated moieties of the nanoparticles as source of $^{19}F^-$ secondary ions for the imaging of influenza hemagglutinin in plasma membranes by high resolution Secondary Ion Mass Spectrometry (SIMS). The system devised by the authors consists in fluorinated nanoparticles (20 nm in diameter) comprising **1** and 11-mercaptoundecanoic acid in their monolayer. Solubility in water was ensured by condensation of lysine with the carboxylic groups on the surface of the nanoparticles. This water-soluble scaffold was further functionalized with a secondary goat anti-mouse antibody obtaining a nanoparticle-based anti-mouse immunolabel. Cells expressing influenza hemagglutinin were pretreated with an anti-hemagglutinin mouse monoclonal antibody and afterwards reacted with the immunolabel. The nanoparticles were found to localize on the plasma membrane in correspondence of the hemagglutinin. NanoSIMS secondary ion imaging analysis of the sample was achieved by detecting $^{19}F^-$ ions. Analysis of the images obtained by monitoring the $^{197}Au^-$ secondary ions confirmed co-localization of the signals.

The complexation properties of gold nanoparticles protected by fluorinated ligands have also been exploited in the development of analytical procedures for the quantitation of perfluoro compounds [40], a subject of increasing concern given the long persistence of these compounds in the environment. In this study the detection of the perfluoro compounds (detection limit down to 20 nM), results from the decrease in solubility of nanoparticles featuring monolayers comprising fluorinated and pegylated thiols upon exposure to the analyte. The reduction of solubility results from the formation of cross-links between different particles that eventually led to precipitation.

Toxicity of fluorous gold nanoparticles.

The toxicity of water-soluble fluorous nanoparticles described in the previous sections is an important aspect that needs to be carefully addressed in order to propose any viable diagnostic and/or therapeutic applications of these systems. At present very little is known in this respect and this lack of information is mainly related to the early stage of the development of these nanostructures that are nowadays mainly tested at the *in vitro* level.

Among the few recent data available, the cytotoxicity of the nanoparticles' vesicles, reported by Niikura and coworkers, was evaluated as control in their studies aimed at assessing the toxicity of the Doxorubicin-loaded vesicles in HeLa cells [37]. In this study, the unloaded vesicles comprising only gold nanoparticles featuring fluorous ligands were found to produce a death rate of less than 5%, while the loaded vesicles produced a death rate of about 50% upon release of the doxorubicin triggered by laser irradiation. In the absence of laser irradiation, the loaded vesicles were found to be non-toxic, producing a cell death rate of about 5%. Another system that was investigated in terms of its cytotoxicity is that of nanoparticles **11b**, that were proposed as ^{19}F MRI contrast agents. Also for this system the toxicity was evaluated in HeLa cells. At a nanoparticles concentration in the range 0.6 μM - 10 μM, the 95% of the cells were found to be viable after uptake of the nanoparticles as determined by cytofluorimetric analysis [36]. However, considering that for MRI applications a very high concentration of equivalent F nuclei (10^{16} - 10^{19} atoms per voxel) has to be reach in the biological system, this investigation should be extended to higher NP concentrations. Despite the paucity of specific toxicity studies, some general information on the toxicity of these systems may be partly inferred from the available data on the toxicity of fluorocarbons, perfluoropolyethers or fluorocarbon-hydrocarbon block copolymers. In fact, these are the structural units employed in the design of the nanoparticles' monolayer and these are the compounds that are expected to be present in the living organisms upon removal of the nanoparticles ~~disruption~~ coting. On the other hand, some studies already displayed that the toxicity of gold nanoparticles bearing hydrogenated ligands correlates with their size [41, 42] and monolayer organization [43]. In discussing the toxicity of these nanosized materials in correlation with the toxicity of their fluorocarbon building blocks, we need to distinguish between acute and long term toxicity. Most past studies dealt with the evaluation of the acute toxicity of fluorocarbons and related compounds because of their use in the development of putative blood substitutes [44]. The acute toxicity of fluorocarbons or fluorocarbon-hydrocarbon block copolymers was evaluated in several animal models including rats, mice and rabbits and, in general, was found to be low [45]. On the other hand, only in recent years the awareness of the increasing persistence in the

environment of technologically relevant fluorinated compounds such as the perfluoroalkanoic and sulfonic acid stimulated a series of studies aimed at understanding their cytotoxicity [46] and long term toxicity in animal models [47,48]. In this respect, it is important to stress that some fluorinated compounds such as the perfluoro alkanoic and perfluorosulfonic acids, indeed display non-negligible long term toxicity. Interesting building blocks in the design of the nanoparticles' monolayer are perfluoropolyethers, these compounds are being extensively studied as ^{19}F MRI tracers *in vitro* and *in vivo* [49-51] and the data support a limited toxicity. Given the low cytotoxicity of these systems, application for cell tracking *in vivo* could be foreseen in analogy to nanoemulsion containing perfluoropolyether (PFPE) described by Ahrens [52, 53].

The information on the acute toxicity is relevant for the application of fluorous nanoparticles for diagnostic purposes, where a single, presumably high, dose is likely to be administered. Instead the information on the long term toxicity could be relevant if the nanosized fluorous materials are intended as therapeutics, for which a prolonged, presumably repeated administration is likely to be necessary. Overall, these information are of great help in leading the design of novel nanoparticle systems, because they allow avoiding the use of any species (or their precursors) of so far known toxicity.

Perspectives

There is increasing evidence that besides the weak interactions between fluorinated species in bulk phases, the fluorophilic interactions may play an important role at the nanoscale. Areas of nanoparticles' research that are witnessing a benefit of a deeper understanding of fluorophilic interactions are the self-assembly of nanosized objects, the development of nanosized carriers for small organic molecules and the surface patterning of gold nanoparticles. Many other applications are probably just around the corner. As far as the self-assembly of nanoparticles driven by fluorophilic interactions is concerned, we expect this approach to be "orthogonal" to any self-assembly process driven by hydrophobic interactions or hydrogen bond formation. In addition, fluorinated species are active components in the formation of halogen bonds [54] which is also complementary to hydrogen bond and hydrophobic interactions, further expanding the diversity of interactions available to the self-assembly of ordered structures. These different levels of orthogonality provide a powerful set of strategies to the construction of ordered structures but their interplay need to be deeply understood in order to evolve from serendipitous discoveries to rational design. Exploiting fluorophilic interactions for molecular recognition proved to be a practicable strategy, establishing that at the nanoascale, confined fluorous phases act as hosting systems with enhanced complexing ability for both

hydrogenated and fluorinated species. The affinity of fluorous mixed monolayers towards small organic molecules depends on the monolayer morphology in a way that cannot be predicted on the basis of the properties of homoligand monolayers requiring the development of novel interpretative models. However, these challenges do not come alone, and a more basic issue remains: the need of developing an understanding of these systems requires a molecular repertoire of fluorous structures capable of co-existing with hydrocarbon in the same milieu.

Acknowledgements

Italian Ministry of Health: project GR-2009-1579849; FIRB prot. RBAP11ETKA, MIUR: Project MULTINANOITA; University of Trieste: FRA 2011 and FRA 2012, and Beneficentia Stiftung.

References

[1] R. Schreiber, J. Do, E.-M. Roller, T. Zhang, V. J. Schüller, P. C. Nickels, J. Feldmann, T. Liedl, Nat. Nanotechnol. 9 (2014) 74–78.

[2] M. Stratakis, H. Garcia, Chem. Rev.112 (2012) 4469–4506.

[3] V. Bijuab, Chem. Soc. Rev. 43 (2014), 744-764.

[4] S. Rana, A. Bajaj, R. Mout, V. M. Rotello, Adv. Drug Deliv. Rev. 64 (2012) 200-216.

[5] C. S. Kim, G.Y. Tonga, D. Solfiell, V. M. Rotello, Adv. Drug Deliv. Rev. 65 (2013) 93–99.

[6] L. Vigderman, E. R. Zubarev, Adv. Drug Deliv. Rev. 65 (2013) 663-676.

[7] J. Sun, Y. Xianyua, X. Jiang, Chem. Soc. Rev. 43 (2014) 6239-6253.

[8] F. Lu, T. L. Doane, J.-J. Zhu, C. Burda, Inorg. Chim. Acta. 393 (2012) 142–153.

[9] M. Brust, M. Walker, D. Bethell, D. J. Schiffrin, R. Whyman, J. Chem. Soc., Chem. Commun. (1994), 801-802.

[10] R. S. Ingram, M. J. Hostetler, R. W. Murray, J. Am. Chem. Soc. 119 (1997) 9175-9178.

[11] A. M. Jackson, J. W. Myerson, F. Stellacci, Nat. Mater. 3, (2004) 330-336.

[12] C. Singh, P. K. Ghorai, M. A. Horsch, A. M. Jackson, R.G. Larson, F. Stellacci, S. C. Glotzer, Phys. Rev. Lett. 99 (2007) 226106.

[13] P. S. Shah, J. D. Holmes, R. C. Doty, K. P. Johnston, B. A. Korgel, J. Am. Chem. Soc. 122 (2000) 4245-4246.

[14] T. Yonezawa, S.-Y. Onoue, N. Kimizuka, Adv. Mater. 13 (2001) 140- 142.

[15] T. Yonezawa, S.-Y. Onoue, N. Kimizuka, Langmuir 17 (2001) 2291-2293.

[16] A. Dass, R. Guo, J. B. Tracy, R. Balasubramanian, A. D. Douglas, R. W. Murray, Langmuir 24 (2008) 310-315.

[17] R. Balasubramanian, R. Guo, A. J. Mills, R. W. Murray, J. Am. Chem. Soc. 127 (2005) 8126-8132.

[18] J. Im, A. Chandekar, J. E. Whitten, Langmuir 25 (2009) 4288–4292.

[19] H. Yang, Y. Wang, H. Huang, L. Gell, L. Lehtovaara, S. Malola, H. Häkkinen, N. Zheng, Nat. Commun. 4 (2013) 2422.

[20] L. Sun, X. Yang, B. Wu, L. Tang, J. Chem. Phys 135 (2011) 204703.

[21] P. S. Shah, S. Husain, K. P. Johnston, B. A. Korgel, J. Phys. Chem. B 105 (2001) 9433–9440.

[22] P. S. Shah, S. Husain, K. P. Johnston, B. A. Korgel, J. Phys. Chem. B. 106 (2002) 12178–12185.

[23] C. Gentilini, M. Boccalon, L. Pasquato, Eur. J. Org. Chem. (2008) 3308–3313.

[24] Gentilini, F. Evangelista, P. Rudolf, P. Franchi, M. Lucarini, L. Pasquato, J. Am. Chem. Soc. 130 (2008) 15678-15682.

[25] L. Abis, L. Armelao, D. Belli Dell'Amico, F. Calderazzo, F. Garbassi, A. Merigo, E. A. Quadrelli, J. Chem. Soc., Dalton Trans. (2001), 2704–2709.

[26] A. C. Templeton, M. J. Hostetler, C. T. Kraft, R. W. Murray, J. Am. Chem. Soc. 120, (1998), 1906-1911.

[27] T. Nishio, K. Niikura, Y. Matsuo, K. Ijiro, Chem. Commun. 46 (2010) 8977–8979.

[28] K. Niikura, N. Iyo, T. Higuchi, T. Nishio, H. Jinnai, N. Fujitani, K. Ijiro, J. Am. Chem. Soc. 134 (2012) 7632–7635.

[29] C. Gentilini, P. Franchi, E. Mileo, S. Polizzi, M. Lucarini, L. Pasquato, Angew. Chem. Int. Ed. 48 (2009) 3060 –3064.

[30] P. Posocco, C. Gentilini, S. Bidoggia, A. Pace, P. Franchi, M. Lucarini, M. Fermeglia, S. Pricl, L. Pasquato, ACS Nano 6 (2012) 7243–7253.

[31] M. Boccalon, S. Bidoggia, F. Romano, L. Gualandi, P. Franchi, M. Lucarini, P. Pengo, L. Pasquato, J. Mater. Chem. B, 3 (2015) 432-439.

[32] R. P. Carney, G. A. DeVries, C. Dubois, H. Kim, J. Y. Kim, C. Singh, P. K. Ghorai, J. B. Tracy, R. L. Stiles, R. W. Murray, S. C. Glotzer, F. Stellacci, J. Am. Chem. Soc. 130 (2008) 798-799.

[33] I. C. Pons-Siepermann, S. C. Glotzer, ACS Nano 6 (2012) 3919–3924.

[34] I. C. Pons-Siepermann, S. C. Glotzer, Soft Matter 8 (2012) 6226-6231.

[35] T. Shirman, R. Kaminker, D. Freeman, M. E. van der Boom, ACS Nano 5 (2011) 6553–6563.

[36] M. Boccalon, P. Franchi, M. Lucarini, J. J. Delgado, F. Sousa, F. Stellacci, I. Zucca, A. Scotti, R. Spreafico, P. Pengo, L. Pasquato, Chem. Commun. 49 (2013) 8794-8796.

[37] K. Niikura, N. Iyo, Y. Matsuo, H. Mitomo, K. Ijiro, ACS Appl. Mater. Interfaces 5 (2013) 3900–3907.

[38] V. Li, A. Y. Chang, T. J. Williams, Tetrahedron 69 (2013) 7741-7745.

[39] R. L. Wilson, J. F. Frisz, W. P. Hanafin, K. J. Carpenter, I. D. Hutcheon, P. K. Weber, M. L. Kraft, Bioconjugate Chem. 23 (2012) 450–460.

[40] H. Niu, S. Wang, Z. Zhou, Y. Ma, X. Ma,Y. Cai, Anal. Chem. 86 (2014) 4170–4177.

[41] E. C. Dreaden, A. M. Alkilany, X. Huang, C. J. Murphy, M. A. El-Sayed Chem. Soc. Rev., 41 (2012) 2740–2779.

[42] A. M. Alkilany, C. J. Murphy, J. Nanopart. Res. 12 (2010) 2313–2333.

[43] S. Sabella, R. P. Carney, V. Brunetti, M. A. Malvindi, N. Al-Juffali, G. Vecchio, S. M. Janes, O. M. Bakr, R. Cingolani, F. Stellacci, P. P. Pompa Nanoscale 6 (2014) 7052–7061.

[44] D. R. Spahn, Crit. Care 3 (1999) R93–R97.

[45] M. P. Krafft, J. G. Riess, Chem. Rev.109 (2009), 1714–1792.

[46] K.B. Wallace, G. E. Kissling, R. L. Melnickc, C. R. Blystone, Toxicol. Lett. 222 (2013) 257–264.

[47] G. B. Post P. D. Cohn , K. R. Cooper, Environ. Res. 116 (2012) 93–117.

[48] A.R. Scialli, A. Iannucci, J. Turim, Regul. Toxicol. Pharmacol. 49 (2007) 195–202

[49] J. M. Janjic, M. Srinivas, D. K. K. Kadayakkara, E. T. Ahrens, J. Am. Chem. Soc. 130 (2008) 2832-2841.

[50] E. T. Ahrens, B. M. Helfer, C. F. O'Hanlon, C. Schirda, Magn. Reson. Med. 72 (2014) 1696–1701.

[51] M. Srinivas, M. S. Turner, J. M. Janjic, P. A. Morel, D. H. Laidlaw, E. T. Ahrens, Magn. Reson. Med. 62 (2009) 747–753.

[52] B. M. Helfer, A. Balducci, A. D. Nelson, J. M. Janjic, R. R. Gil, P. Kalinski, I. J. M. De Vries, E. T. Ahrens, R. B. Mailliard, Cytotherapy 12 (2010) 238–250.

[53] M. Srinivas, P. A. Morel, L. A. Ernst, D. H. Laidlaw, E. T.Ahrens, Magn. Reson. Med. 58 (2007) 725–734.

[54] G. R. Desiraju, P. S. Ho, L. Kloo, A. C. Legon, R. Marquardt, P. Metrangolo, P. Politzer, G. Resnati, K. Rissanen, Pure Appl. Chem. 85 (2013) 1711–1713.